

# High-spatial-resolution quantum-well intermixing process in GaInAs/GaInAsP laser structure using pulsed-photoabsorption-induced disordering

T. K. Ong, O. Gunawan, B. S. Ooi,<sup>a)</sup> Y. L. Lam, Y. C. Chan, and Y. Zhou  
*Photonics Research Group, School of Electrical and Electronics Engineering,  
Nanyang Technological University, Singapore 639798*

A. Saher Helmy and J. H. Marsh  
*Optoelectronics Research Group, Department of Electronics and Electrical Engineering,  
University of Glasgow, Glasgow G12 8QQ, Scotland, United Kingdom*

(Received 21 June 1999; accepted for publication 13 December 1999)

Raman spectroscopy was used to study the spatial resolution of pulsed-photoabsorption-induced quantum-well intermixing in a GaInAs/GaInAsP laser structure. A differential band gap shift of up to 60 meV has been obtained from a sample masked with  $\text{Si}_x\text{N}_y/\text{Au}$  and exposed to the laser irradiation. Intermixing was detected in the irradiated regions through the shift of GaAs-like modes to lower frequencies. In addition, the intermixing induced GaInP longitudinal optical modes in the irradiated regions, which is evidence of the intermixing between the upper GaInAs cap and the GaInAsP layer. The spatial resolution of this process, which was obtained from micro-Raman spectra when scanned across the interface of the intermixing mask, was found to be better than 2.5  $\mu\text{m}$ . © 2000 American Institute of Physics. [S0021-8979(00)04106-2]

## I. INTRODUCTION

Quantum-well intermixing (QWI)<sup>1</sup> is a promising technique for postgrowth band gap modification of quantum wells (QWs) for the fabrication of photonic integrated circuits. QWI techniques in III–V QW structures such as impurity-free-vacancy disordering,<sup>2</sup> impurity-induced disordering,<sup>3</sup> implantation-defect-induced intermixing,<sup>4</sup> and laser-induced disordering (LID)<sup>5</sup> have been reported. Among these techniques, LID techniques are attractive as they are impurity free and offer the possibility of a direct writing capability.<sup>6</sup>

Photoabsorption-induced disordering (PAID) using a continuous wave (cw) Nd:YAG laser is an example of a LID technique developed in the GaInAs/GaInAsP QW system. It involves band-to-band absorption of the incident cw laser radiation wavelength within the active region. Subsequent carrier cooling and nonradiative recombination result in the generation of heat, causing interdiffusion of the QW layers to take place. The lateral spatial resolution of the PAID process was found to be  $\sim 100 \mu\text{m}$ , which resulted in poor performance of monolithically integrated photonic devices.<sup>7,8</sup> Pulsed-photoabsorption-induced disordering (P-PAID) is another LID technique, which potentially offers better spatial resolution. In this process, a Q-switched Nd:YAG laser with a pulse length of  $\sim 8$  ns and a repetition rate of 10 Hz is typically used to irradiate the sample directly. The absorption of high-energy pulses from the Nd:YAG laser causes bond breaking and lattice disruption in the sample, which lead to an increase in the point defect density. Subsequent high temperature annealing results in diffusion of the point defects and enhances the QWI rate. Using spatially resolved photoluminescence (PL) spectroscopy measurements, a spatial

resolution of  $< 25 \mu\text{m}$  has been determined.<sup>9</sup> In addition, time resolved photoluminescence (TRPL) measurements carried out on the same sample indicated a spatial resolution of  $< 20 \mu\text{m}$ .<sup>10</sup>

Aside from PL and TRPL measurements, Raman scattering is also one of the tools conventionally used to characterize the III–V semiconductors. Raman spectroscopy has been used to study the interdiffusion mechanism in QWs and superlattices (SLs).<sup>11–15</sup> In particular, in GaInAs/InP SLs, it was demonstrated that the peak intensities and peak energies of the InAs-, GaAs-, and InP-like longitudinal optical (LO) phonon modes change with annealing temperature and time.<sup>13</sup> The effect of thermal interdiffusion on a single quantum well (SQW) in GaInAs/GaInAsP has been investigated.<sup>14</sup> The quaternary QW structure exhibits two large groups of bands associated with LO phonons in the barriers and the well respectively which makes the analysis of the spectra complicated.

Here we report the observation of a large differential band gap shift between  $\text{Si}_x\text{N}_y/\text{Au}$  masked and exposure region in a GaInAs/GaInAsP SQW laser structure obtained using the P-PAID technique. The spatial resolution of this technique was studied using micro-Raman spectroscopy by scanning across masked and intermixed interfaces.

## II. EXPERIMENT

The GaInAs/GaInAsP SQW laser structure used in this experiment was grown by metalorganic chemical vapor deposition on an S-doped InP substrate. Figure 1 shows the overview of the layer structure.

A 200 nm thick  $\text{Si}_x\text{N}_y$  layer was first deposited on the sample using plasma-enhanced chemical vapor deposition. This dielectric layer acts as an antireflection coating as well as a protective layer against surface reaction with the atmo-

<sup>a)</sup>Electronic mail: ebsooi@ntu.edu.sg

$1.8 \times 10^{19} \text{ cm}^{-3}$ Zn-doped	$\text{Ga}_{0.47}\text{In}_{0.53}\text{As}$	100 nm	Contact layer
$2.0 \times 10^{18} \text{ cm}^{-3}$ Zn-doped	$\text{Ga}_{1-x}\text{In}_x\text{As}_y\text{P}_{1-y}$ ( $\lambda_g=1.18$ )	50 nm	
$7.3 \times 10^{17} \text{ cm}^{-3}$ Zn-doped	InP	1370 nm	Upper cladding
undoped	$\text{Ga}_{1-x}\text{In}_x\text{As}_y\text{P}_{1-y}$ ( $\lambda_g=1.05$ )	80 nm	Graded index structure
undoped	$\text{Ga}_{1-x}\text{In}_x\text{As}_y\text{P}_{1-y}$ ( $\lambda_g=1.18$ )	50 nm	
undoped	$\text{Ga}_{1-x}\text{In}_x\text{As}_y\text{P}_{1-y}$ ( $\lambda_g=1.26$ )	12 nm	Barrier
undoped	$\text{Ga}_{0.47}\text{In}_{0.53}\text{As}$	5.5 nm	Quantum well
undoped	$\text{Ga}_{1-x}\text{In}_x\text{As}_y\text{P}_{1-y}$ ( $\lambda_g=1.26$ )	12 nm	Barrier
$5.0 \times 10^{17} \text{ cm}^{-3}$ S-doped	$\text{Ga}_{1-x}\text{In}_x\text{As}_y\text{P}_{1-y}$ ( $\lambda_g=1.18$ )	50 nm	Graded index structure
$5.0 \times 10^{17} \text{ cm}^{-3}$ S-doped	$\text{Ga}_{1-x}\text{In}_x\text{As}_y\text{P}_{1-y}$ ( $\lambda_g=1.05$ )	80 nm	
$2.5 \times 10^{18} \text{ cm}^{-3}$ S-doped	InP	1000 nm	Lower cladding
$3.8 \times 10^{18} \text{ cm}^{-3}$ S-doped	InP substrate		

FIG. 1.  $\text{Ga}_{1-x}\text{In}_x\text{As}/\text{Ga}_{1-x}\text{In}_x\text{As}_y\text{P}_{1-y}$  SQW laser structure used in the experiment.  $\lambda_g$  is the room temperature PL wavelength in  $\mu\text{m}$ .

sphere. A 200 nm gold mask was then evaporated and defined on the  $\text{Si}_x\text{N}_y$  surface using photolithography and lift-off. The sample was irradiated using a Q-switched 1.064  $\mu\text{m}$  Nd:YAG laser with a pulse energy density of 3.0  $\text{mJ mm}^{-2}$  for 2 min at room temperature and at normal incidence to the surface. The pulse width of the laser was  $\sim 8$  ns and the pulse repetition rate was 10 Hz. The sample preparation for the experiment is shown in Fig. 2.

The gold mask was lifted off using hydrofluoric acid after laser exposure. The QWI stage was carried out using a rapid thermal processor at 625  $^\circ\text{C}$  for 120 s. During annealing, the sample was sandwiched between two pieces of fresh GaAs substrate to provide an As overpressure. PL measurements were performed at 77 K on both the masked and exposed regions before and after annealing to access the degree of QWI. The PL spectra are shown in Fig. 3. The PL spectrum from the masked region shows a wavelength shift of only 2.5 meV compared to that of the as-grown samples, whereas the unmasked region has an additional blueshift of about 60 meV. From the PL spectra, it is deduced that the gold mask can be used as a beam reflector to prevent the laser beam from entering the sample. The laser pulses will

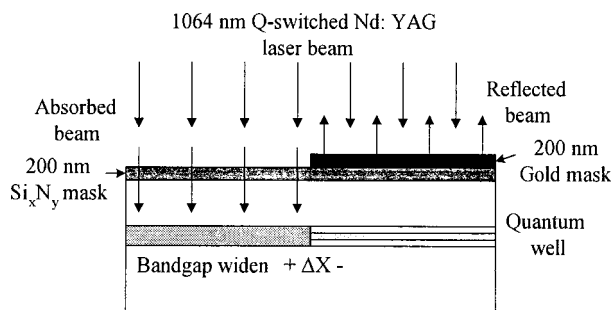


FIG. 2. Sample preparation for the spatial resolution experiment.

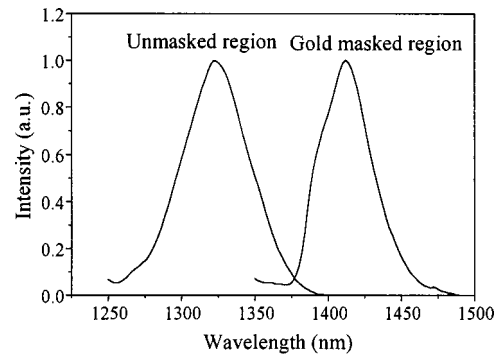


FIG. 3. Normalized PL emission spectra from the gold masked and unmasked regions.

only be absorbed in the unmasked region, hence generating point defects. These point defects will in turn diffuse during subsequent high temperature annealing, thus resulting in the QWI. The band gap energy of the QW in the unmasked region is therefore expected to increase compared to that of the gold masked region.

To investigate the spatial resolution of the process, micro-Raman spectra were taken in the backscattering configuration in 2.5  $\mu\text{m}$  increments across the interface of the intermixing mask. During the Raman measurements, the number of data-set averages was set to three to improve the signal-to-noise ratio. The sample was positioned and aligned on a high-precision  $x$ - $y$ - $z$  translation stage and the measurements were carried out at room temperature. An  $\text{Ar}^+$  laser operating at a wavelength of 514.5 nm, 20 mW power, and with a spot diameter of  $\leq 1 \mu\text{m}$  was used as excitation source. The penetration depth of the light, calculated from its absorption length in the structure, is about 50 nm below the sample surface.<sup>16</sup>

### III. RESULTS AND DISCUSSION

Due to the laser excitation source and the structure used, the Raman modes with the largest signal-to-noise ratio generated in these measurements are those of the GaInAs contact layer, rather than the QW layer. The P-PAID process generates point defects not only throughout the active region but also in the cap. The highest concentration of point defects is expected in the cap because of the intensity of the beam and the nonlinear nature of the process. The spatial resolution is determined by the localization with which point defects can be created, and the distance they diffuse during the annealing step. Any difference in spatial resolution between intermixing in the cap and QW layers should, to a first approximation, only depend on diffraction of the beam in the region between the cap and the active region, which is a distance of about 1.5  $\mu\text{m}$ . The spatial resolution of intermixing in the GaInAs cap layer is therefore expected to be similar to that in the QW. If the spatial resolution of the process is obtained for the top contact layer, it should be of the same order to that of the QW.

Figure 4 shows the Raman spectra taken in steps of 2.5  $\mu\text{m}$  across the gold masked boundary, as shown in Fig. 2. For comparison, the spectrum from an as-grown sample is

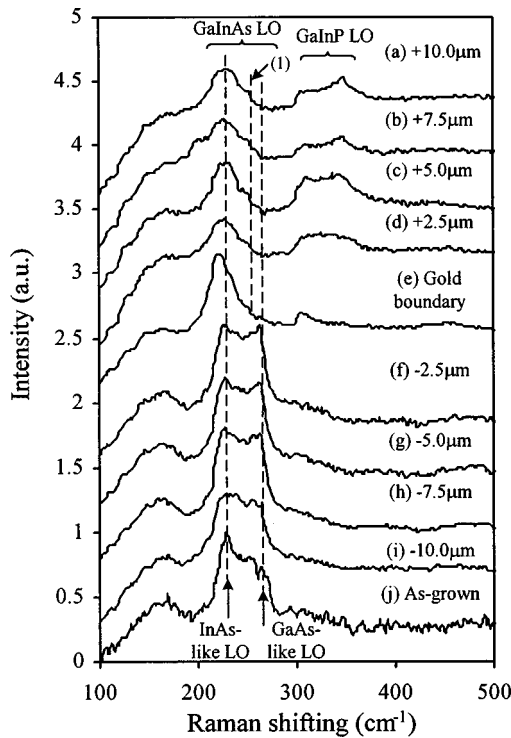


FIG. 4. Raman spectra measured in steps of +2.5 and -2.5 μm from the gold masked boundary.

also included. Since the sample was grown with (100) orientation, only longitudinal optical phonons are allowed and the transverse optical phonons are forbidden by symmetry selection rules. Three groups of bands can be identified in the spectra. The low frequency range (<200 cm<sup>-1</sup>) band is assigned to the disorder activated longitudinal acoustic (DALA) mode that is found in III-V alloy crystals.<sup>15</sup> The two higher frequency bands in the 210–270 and 300–370 cm<sup>-1</sup> frequency ranges are identified as optical modes. The 210–270 cm<sup>-1</sup> band corresponds to the GaInAs-related LO mode. This band is composed of InAs-like (210–235 cm<sup>-1</sup>) and GaAs-like (240–270 cm<sup>-1</sup>) LO peaks. The band at around 300–370 cm<sup>-1</sup> is interpreted as arising from the GaInP LO mode. The measured LO phonon frequencies as a function of distance from the gold masked boundary are summarized in Fig. 5.

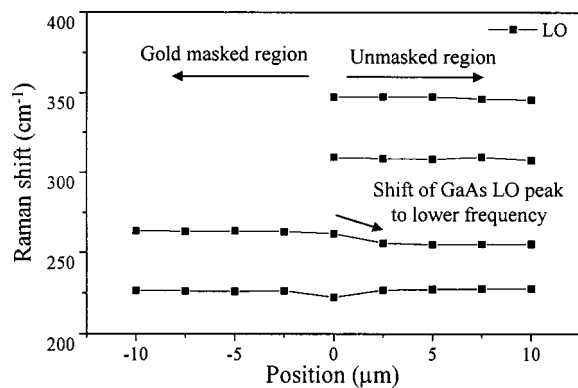


FIG. 5. Measured LO phonon frequencies as a function of distance from the gold masked boundary.

Three distinct types of spectra can be observed in Fig. 4.

(1) The spectra in Figs. 4(a)–4(d) were obtained from the laser-irradiated, and hence, intermixed region. The most distinctive differences between the spectra from this intermixed region compared to those of the as-grown [Fig. 4(j)] and gold masked region [Figs. 4(f)–4(i)] are the shift of the GaAs-like LO peak of ~8 cm<sup>-1</sup> to the lower frequency (line 1) and the reduction of its intensity. The clear shift to a lower frequency and the decrease of intensity of the GaAs-like LO peak are indications for the compositional change in the Ga<sub>1-x</sub>In<sub>x</sub>As layer due to the out-diffusion of the Ga and As.<sup>13</sup> The Ga and As vacancies are then replaced by In and P from the Ga<sub>1-x</sub>In<sub>x</sub>As<sub>y</sub>P<sub>1-y</sub> layer which is located directly under the Ga<sub>1-x</sub>In<sub>x</sub>As layer, thus converting the top Ga<sub>1-x</sub>In<sub>x</sub>As layer into Ga<sub>1-x</sub>In<sub>x</sub>As<sub>y</sub>P<sub>1-y</sub>. This postulate is further supported through the intensity of the GaInP band (300–370 cm<sup>-1</sup>), which becomes one of the dominant bands in the irradiated region. In these spectra, the DALA modes are also substantially reduced in comparison to those of the as-grown sample. This suggests that the disordering evident in the as-grown sample is annealed out during processing.

(2) The spectrum in Fig. 4(e) was measured from the gold masked boundary. Because it is the transitional region, it carries features resembling both the intermixed and as-grown spectra. The GaAs-like mode was found to shift to the lower frequency, similar to the shift in the irradiated region, while the InAs-like LO peak shows a shift of ~4 cm<sup>-1</sup> to the lower frequency. The GaInP band (300–370 cm<sup>-1</sup>) starts to increase at this boundary although the intensity is lower than that observed in the irradiated region. In addition, the DALA modes could be seen, in this spectrum, are similar to that of the as-grown sample.

(3) The spectra in Figs. 4(f)–4(i) were taken from the gold masked region. In these spectra, the GaInAs LO modes are also the only ones observed. Both the GaAs-like and the InAs-like modes remain distinguished, which agrees well with the minimal intermixing observed in this region. Moreover, these Raman spectra, which are very similar to those observed in the as-grown sample, indicate the lack of any noticeable intermixing between the GaInAs cap and the GaInAsP layer after annealing in the masked regions. This is also clearly evident in the wavelength of the PL peak with a shift of only 2.5 meV compared to that of the as-grown samples. In this region, similar to the as-grown sample, the DALA modes are clearly shown.

After analyzing the Raman spectra, it is clear that the change of the Raman peaks between the intermixed and unintermixed regions takes place between two consecutive Raman spectra measurements, which are 2.5 μm apart. This implies that the resolution of the P-PAID process at the GaInAs cap is better than 2.5 μm. However, as discussed above, the resolution at the QWs should be in the same order.

The shift to lower frequency and the decrease of the intensity of the GaAs-like LO mode in the unmasked region are ascribed to the increase in the In concentration (x) due to the interdiffusion of the group III and group V elements between the Ga<sub>1-x</sub>In<sub>x</sub>As and Ga<sub>1-x</sub>In<sub>x</sub>As<sub>y</sub>P<sub>1-y</sub> layers. Com-

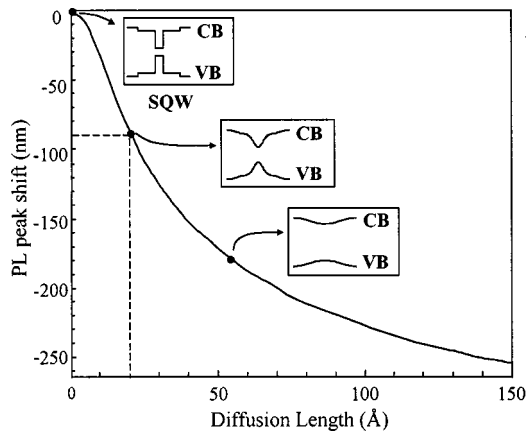


FIG. 6. Calculated PL wavelength shift with respect to as-grown at various diffusion lengths. The insets show the QW band gap profile for three different group III diffusion lengths.

paring the shifted frequency of the GaAs-like LO mode with the results reported by Sugiura *et al.* and Soni *et al.*, the  $y$  composition is approximated to 0.79.<sup>12,17</sup> Assuming conservation of the lattice matching condition ( $x = 1 - 0.47y$ ),<sup>18</sup> the expected  $x$  composition resulting from the intermixing will be  $\sim 0.63$ . Bound states of the intermixed  $\text{Ga}_{1-x}\text{In}_x\text{As}/\text{Ga}_{1-x}\text{In}_x\text{As}_y\text{P}_{1-y}$  QW can be calculated using the error-function model.<sup>19</sup> Figure 6 shows the calculated excitonic peak shift with respect to the diffusion length of the QW that characterizes the degree of intermixing in the QW. The plot is generated from a series of bound states calculation of electron and holes confined in the QW using Ben-Daniel Duke's equation in the effective mass approximation. Assuming the lattice matching condition, the As concentration ( $y$ ) in the middle of the QW ( $z=0$ ) can be calculated at various diffusion lengths as given in Fig. 7. From the PL measurement at 77 K, the PL shift of the excitonic peak will correspond to a certain value of diffusion length. Then the value of the As composition in the middle of the QW ( $y$ ) can be obtained from Fig. 7. Therefore, using Figs. 6 and 7, the corresponding As concentration ( $y$ ) due to a PL peak shift of 90 nm obtained from Fig. 3 is  $\sim 0.83$  which is close to that predicted from the Raman spectroscopy measurements.

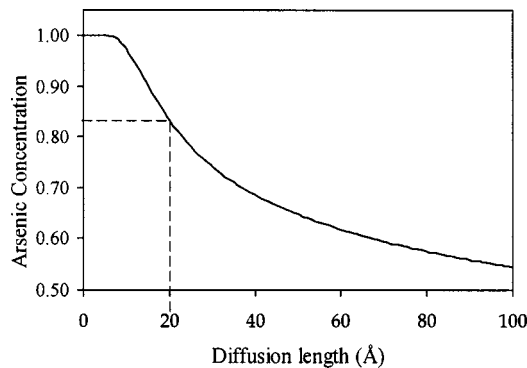


FIG. 7. As concentration in the middle of the QW.

#### IV. CONCLUSION

The spatial resolution of the P-PAID QWI technique has been studied using micro-Raman spectroscopy on a GaInAs/GaInAsP SQW laser structure. A differential band gap shift of 60 meV has been obtained across a single sample, when a  $\text{Si}_x\text{N}_y/\text{Au}$  mask was used to prevent exposure to the laser irradiation in selected areas. Gold was therefore proven to be an effective reflector and, hence, mask for the P-PAID technique. By acquiring Raman spectra from the cap whilst scanning across the intermixed and masked regions, it was deduced that the spatial resolution of this process is at least  $2.5 \mu\text{m}$ , limited by the measurement setup. In the irradiated regions the intermixing induces GaInP LO modes, which verify the intermixing between the upper GaInAs cap and the GaInAsP layer. In these regions the intermixing is also evident in the shift of GaAs-like modes to lower frequencies indicating the out-diffusion of the Ga and As and their replacement with In and P. The corresponding change of the As concentration ( $y$ ) after the intermixing has also been calculated.

#### ACKNOWLEDGMENTS

The authors wish to thank Professor Hui Ping and George Chen at Photonics Research Laboratory, Nanyang Technological University, for providing access to the Q-switched Nd:YAG laser. They are grateful to Professor X. Shi and J. R. Shi at Ion Beam Processing Laboratory, Nanyang Technological University, for assisting in the Raman spectroscopy measurements. This work was supported by Academic Research Funds, Ministry of Education (Singapore) under Grant Nos. RG47/96 and RG 18/97.

- <sup>1</sup>J. H. Marsh, *Semicond. Sci. Technol.* **8**, 1136 (1993).
- <sup>2</sup>B. S. Ooi, K. McIlvaney, M. W. Street, A. Saher Helmy, S. G. Ayling, A. C. Bryce, J. H. Marsh, and J. S. Roberts, *IEEE J. Quantum Electron.* **33**, 1784 (1997).
- <sup>3</sup>D. G. Deppe and N. Holonyak, Jr., *J. Appl. Phys.* **64**, R93 (1988).
- <sup>4</sup>J. Cibert, P. M. Petroff, D. J. Werder, S. J. Pearton, A. C. Gossard, and J. H. English, *Appl. Phys. Lett.* **49**, 223 (1986).
- <sup>5</sup>C. J. McLean, J. H. Marsh, R. M. De La Rue, A. C. Bryce, B. Garrett, and R. W. Glew, *Electron. Lett.* **28**, 1117 (1992).
- <sup>6</sup>B. S. Ooi, E. L. Portnoi, C. J. McLean, A. McKee, C. C. Button, A. C. Bryce, R. M. De La Rue, and J. H. Marsh, *IPRM'96 Conference, Proceedings of the Eighth International Conference on InP and Related Material, Schwäbisch Gmünd 1996, Vol. 8, p. 252.*
- <sup>7</sup>C. J. McLean, A. McKee, J. H. Marsh, and R. M. De La Rue, *Electron. Lett.* **29**, 1657 (1993).
- <sup>8</sup>A. McKee, C. J. McLean, G. Lullo, A. C. Bryce, R. M. De La Rue, J. H. Marsh, and C. C. Button, *IEEE J. Quantum Electron.* **33**, 45 (1997).
- <sup>9</sup>C. J. McLean, A. McKee, G. Lullo, A. C. Bryce, R. M. De La Rue, and J. H. Marsh, *Electron. Lett.* **31**, 1285 (1995).
- <sup>10</sup>S. J. Fancey, G. S. Buller, J. S. Massa, A. C. Walker, C. J. McLean, A. McKee, A. C. Bryce, J. H. Marsh, and R. M. De La Rue, *J. Appl. Phys.* **79**, 9390 (1996).
- <sup>11</sup>A. Pinzuk, J. M. Worlock, R. E. Nahory, and M. A. Pollack, *Appl. Phys. Lett.* **33**, 461 (1978).
- <sup>12</sup>T. Sugiura, N. Hase, Y. Iguchi, and N. Sawaki, *Jpn. J. Appl. Phys., Part 1* **37**, 544 (1998).
- <sup>13</sup>S. J. Yu, H. Asahi, S. Emura, S. I. Gonda, and K. Nakashima, *J. Appl. Phys.* **70**, 204 (1991).



- <sup>14</sup>H. Pyre, F. Alsina, J. Camassel, J. Pascual, and R. W. Glew, *J. Appl. Phys.* **73**, 3760 (1993).
- <sup>15</sup>T. Inoshita, *J. Appl. Phys.* **56**, 2056 (1984).
- <sup>16</sup>H. Burkhard, H. W. Dinges, and E. Kuphal, *J. Appl. Phys.* **53**, 655 (1982).
- <sup>17</sup>R. K. Soni, S. C. Abbi, K. P. Jain, M. Balkanski, S. Slemple, and J. L. Benchimol, *J. Appl. Phys.* **59**, 2184 (1986).
- <sup>18</sup>S. Adachi, *J. Appl. Phys.* **53**, 8775 (1982).
- <sup>19</sup>J. Micallef, E. H. Li, and B. L. Weiss, *J. Appl. Phys.* **73**, 7524 (1993).